BONDED REPAIRS OF COMPOSITE STRUCTURES: VOID FORMATION MECHANISMS IN AN ADHESIVE FILM

M. Préau, N. Auda-Kothari, and P. Hubert*

Structures and Composite Materials Laboratory, Department of Mechanical Engineering,
McGill University, 817 rue Sherbrooke Ouest, MacDonald Bldg, Montreal, H3A 0C3, QC, Canada
*Corresponding author (pascal.hubert@mcgill.ca)
http://www.composite.mcgill.ca

Keywords: Adhesive Bonding, Out-of-Autoclave, Moisture, Porosity, Modelling

Abstract

With the increasing use of composite materials in aerospace structures, the interest for reliable repair processes is growing. Scarf co-bonded repairs are typically carried out using a thermoset adhesive film and repair plies that are consolidated under vacuum pressure only (1 atm). Additionally, in a repair environment, adhesive films are sensitive to moisture uptake at room temperature, and pre-bond moisture may be present within the structure to be repaired. Under the condition of reduced compaction pressure, the presence of pre-bond moisture may generate voids in the adhesive by off-gassing dissolved species such as water.
In this paper, the causes and mitigation of porosity in adhesive bonding are discussed with the support of an experimental characterization of void evolution compared to a diffusion-based model. First, the adhesive cure kinetic, rheological behaviour and volatile evolution are characterized. Then, to simulate ideal and deficient repair conditions, various moisture contents were tested experimentally on an adhesive film, and void evolution was monitored under an instrumented glass tool-plate. The results show that small amount of absorbed water may lead to void growth within an adhesive under ambient consolidation pressure. Overall, the void growth measurements throughout the cure were found to correlate well with model predictions.

1. Introduction

1.1. Background

The growing share of composite materials in primary structures of commercial aircraft pushes the need for cost-effective, reliable, and durable repair methods in the manufacturing and maintenance industry. While bonded repair methods are attractive in comparison to heavy bolted repairs, they lack robustness for airworthy certification other than for cosmetic repairs [1]. Co-bonded repairs provide a high property recovery solution, but their quality and subsequent performance are highly process-dependent. Indeed, repairs are performed directly on a component under atmospheric consolidation pressure only (out-of-autoclave), with possible contamination. In this context, the presence of voids or porosity is typically high, and 5–10 % of porosity is not uncommon in wet-lay-up [2] and prepreg repairs [3]. This is a major concern for repairing load-bearing structures since porosity significantly reduces tensile [4] and compressive [3] strength recovery, fatigue life [5], and also largely impairs the detectability of defects with non-destructive ultrasonic methods [6].

Excerpt from ISBN 978-3-00-053387-7

The two main sources of porosity in adhesive bonding are reported to be: entrapped air and solvent/water off-gassing [1]. Entrapped air was found to be successfully mitigated in vacuum bag only processing with the use of a textured adhesive film [4]. Because the presence of moisture in a repair environment is a common challenge, the focus of this paper is on understanding the conditions of void growth induced by off-gassing of absorbed water [7]. Moisture ingress may come from either insufficient drying prior to bonding [8] or ambient humid air. Additionally, depending on void stability conditions, the limited available consolidation pressure with vacuum bag only repair processes may not be sufficient to keep dissolved species in solution within the adhesive and prevent void expansion, leading to rapid void evolution at elevated temperatures [9].

1.2. Objective and Approach

The objective of this paper is to predict the onset of void growth and final void content in an adhesive under various processing conditions of humidity and pressure. First, the adhesive film cure kinetics and rheological behaviours are briefly presented along with the off-gassing behaviour of the material during cure. Then, a diffusion-based model is introduced with the characterization of model input parameters. Finally, the model is compared and validated with void growth measurements by means of an instrumented glass tool-plate.

2. Materials and Experimental Methodology

2.1. Materials

The adhesive considered for this study was a toughened epoxy B-staged adhesive film: Cytec FM® 300-2M. This common repair adhesive film has an areal weight of 293 g/m^2 and a nominal thickness of 0.25 mm. The film also features a non-woven polyester carrier aiming at improving handling and bondline thickness control.

2.2. Thermal Characterizations

The exothermic reaction and viscosity were measured respectively by a DSC Q100 and a rheometer AR 2000 (both from TA Instruments). For each test, dynamic runs at 1, 2 and 3 °C/min and isothermal tests at 80, 100, 120 and 140 °C were carried out following the procedures described in [10]. To identify the volatile content and release evolution, a Linseis PT 1600 TGA coupled with an IR spectrometer (Nicolet 6700) was used on a 13 g adhesive specimen conditioned under 90 %RH until saturation. For this test, the recommended cure cycle was used: 2 °C/min to 121°C for an hour.

2.3. Instrumented Glass Tool-plate Experiments

A transparent glass tool-plate fixture was used, as shown in the schematic of Figure 1, to monitor void evolution in the adhesive film under various processing conditions. After the samples were equilibrated under the relative humidity conditions, a 25 × 55 mm adhesive film was placed between the released glass-tool plate and a glass lamellae, followed by a non-perforated release film, a PID-controlled heat blanket providing heat, breather and the vacuum bag.

Real-time visualizations of void formation and growth were tracked by a digital Dino-lite camera (AM 70130 ZT 5) and pictures were taken with the software Dino-Capture throughout each test. A single area of interest was observed for each trial throughout the cure. After gelation, 5 additional pictures were taken in other areas of the sample to assess the variability in porosity across the specimen. Void size, shape, distribution and content were subsequently analyzed with the image processing software ImageJ.

Excerpt from ISBN 978-3-00-053387-7

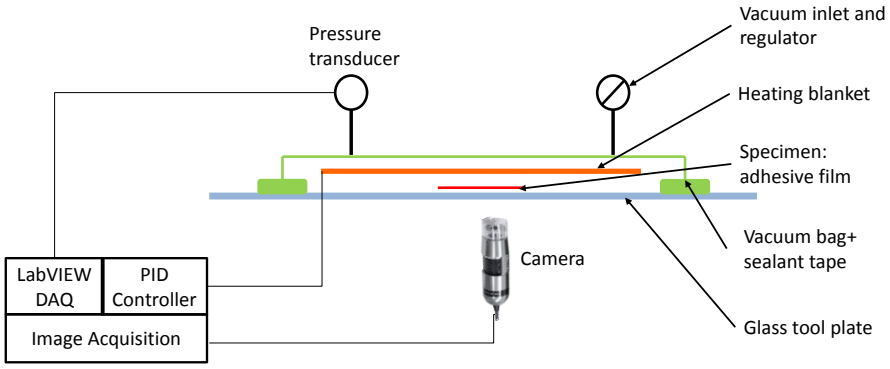

Figure 1 : Schematic of the glass tool-plate experimental setup used to monitor void formation and evolution throughout the adhesive cure. For sack of clarity, thermocouples, the glass lamellae, release films and breather are not shown in this schematic.

3. Void Growth Modelling

3.1. Void Evolution Model

Various researchers have studied the dynamics of spherical bubble growth in an infinite medium, and they have formulated the governing water transfer equations used in this study [9, 11-14]. These models approaches were used to predict void evolution for autoclave cure of various thermoset composite [9, 13, 14], and also were later successfully applied to forecast final void content in partially impregnated prepreg materials in vacuum bag only processing [12]. The model used here is a simplified version of the model of Wood and Bader [11], that neglects surface tension effects, similarly to the approach taken by Kardos, *et al.* [9]. The model gives the evolution of a bubble diameter as a function of time, pre-bond moisture concentration, and applied temperature and pressure on the adhesive film. To the best of our knowledge, this is the first time such model is applied to study void formation and growth in adhesive bonding under ambient consolidation pressure only.

3.2. Model Parameters Characterization and Adhesive Conditioning

The main model input parameters needed for the void growth model are the water diffusivity in the uncured adhesive as a function of temperature, and the water solubility at various levels of relative humidity. Both parameters were experimentally determined by conditioning the adhesive in a 6-litre glass conditioning chamber for 70 and 90 %RH, respectively using a saturated NaCl water solution and tap water to generate the desired relative humidity conditions. A wireless humidity sensor, BLE sensor tag WPP100B001 [15] with a humidity sensor HTU21D(F) from Measurement Specialities [16], was used to monitor and record ambient temperature and relative humidity levels. The adhesive weight mass evolution under the various humidity conditions was measured with a 0.01 mg precision analytical balance (Sartorius CP225D). Diffusion coefficient at different room temperatures (up to 30 °C) were calculated following the procedure detailed in [17].

4. Results

4.1. Thermal Behaviours Modelling and Off-gassing Characterization

The cure behaviour of the adhesive film was measured and a phenomenological model was used to predict the cure kinetics of the adhesive film. Cole, *et al.* [18] model was used to account the diffusion controlled reaction after gelation observed experimentally, and the cure rate model is given by equation (1):

Excerpt from ISBN 978-3-00-053387-7

$$\left(\frac{\delta\alpha}{\delta t}\right) = f(T) = A\,exp\left(\frac{-E_A}{RT}\right)\frac{\alpha^m(1-\alpha)^n}{1+exp\left(C\left(\alpha-(\alpha_{C0}+\alpha_{CT}T)\right)\right)} \quad (1)$$

The model used to describe the adhesive viscosity behaviour is based on the work of Khoun, *et al.* [19] that suggested a second Arrhenius temperature dependency term and a supplementary polynomial term to enhance the viscosity prediction near gelation. The rheological model depends on the cure kinetics and temperature, and is given by equation (2):

$$\mu = g(T,\alpha) = A_{\mu1}exp\left(\frac{-E_{\mu1}}{RT}\right) + A_{\mu2}exp\left(\frac{-E_{\mu2}}{RT}\right)\left(\frac{\alpha_{gel}}{\alpha_{gel}-\alpha}\right)^{A+B\alpha+C\alpha^2} \quad (2)$$

The degree of cure at gelation was determined as the average of the degree of cure for which tan(δ) = 1 for all tests. Activation energies and pre-exponential factors were determined similarly to [10]. For each model, the other constants were calculated using the least squares curve fit with the experimental data, and the input parameters are summarized in the Table 1.

Table 1. Cure kinetics and chemorheological model parameters for FM® 300-2M.

Cure kinetics model - equation (1)

A (s^{-1})	E_A (J/mol)	m	n	C	α_{C0}	α_{CT} (K^{-1})
3.37×10^{10}	9.54×10^{4}	0.92	2.41	25.00	-1.18	5.10×10^{3}

Rheological model - equation (2)

$A_{\mu1}$ (Pa.s)	$E_{\mu1}$ (J/mol)	$A_{\mu2}$ (Pa.s)	$E_{\mu2}$ (J/mol)	α_{gel}	A	B	C
2.02×10^{-10}	7.93×10^{4}	41.0	3.65×10^{3}	0.77	0.10	0.60	2.40

Figure 2 shows the measured cure kinetics and viscosity behaviours compared to the model predictions for FM® 300-2M. For the cure kinetics (A), the model fitted very well the experimental data. For isothermal (B) and dynamic (C) viscosity tests, gel time was also well captured by the model when the degree of cure reaches 77 %. Interestingly, the dynamic rheological tests clearly showed that the minimal viscosity depends on heat rate, with faster heat ramps found to lower the minimum viscosity prior to gelation in Figure 2 (C). For example, at 1 °C/min, the adhesive viscosity reached a minimum viscosity of 275 ± 11 Pa.s, whereas faster heat ramp of 2 °C/min attained 200 ± 5 Pa.s, down to 105 ± 6 Pa.s for 3 °C/min. While the model predictions captured well this trend, they slightly underestimated the minimum viscosity measurements for low heat rates.

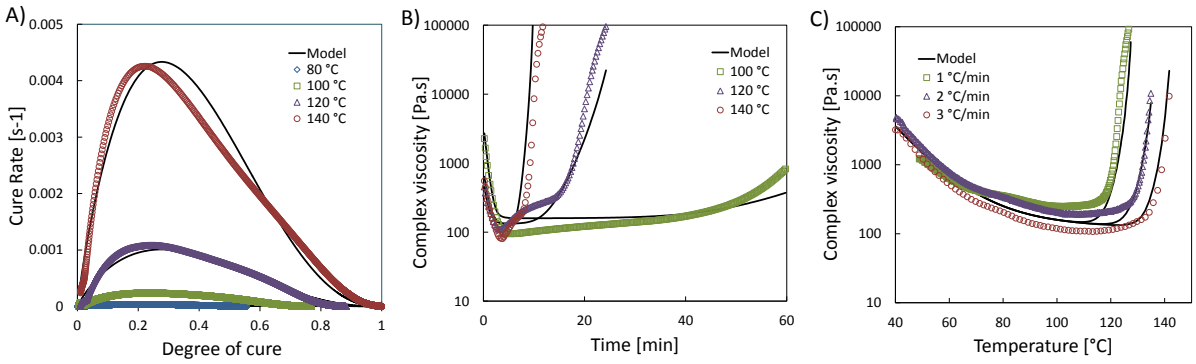

Figure 2 : Charts showing how the cure kinetic and rheology data (symbols) compare to model predictions (solid lines). A) shows cure rate as a function of degree of cure. Isothermal viscosity tests are presented in B), and dynamic viscosity tests are shown in C).

Excerpt from ISBN 978-3-00-053387-7

Then, TGA-FTIR provided insightful information of the nature and release temperature of the off-gassing species for a conditioned adhesive in a humid environment. Measured weight loss was than 1 wt. % up to gelation, which is in accordance with the adhesive film manufacturing data sheet. Figure 3 clearly shows two phases of off-gassing release. A first compound was observed from 67 °C to the temperature hold at 121 °C, recognized as Methyl Ethyl Ketone or MEK. A second distinctive IR spectrum, corresponding to water release, was also being detected around 100 °C until the end of the test.

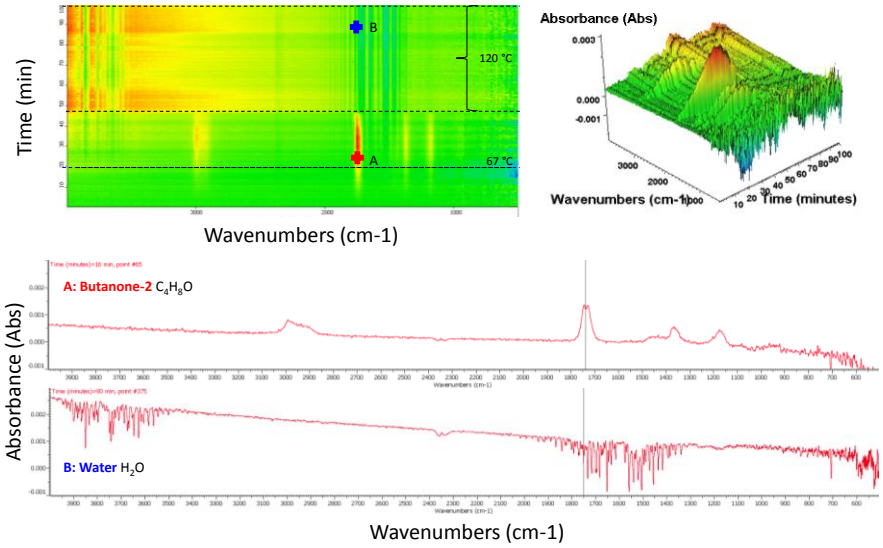

Figure 3 : FTIR data-set during cure represented at a 3D view (top right) and 2D view (top left) with the absorbance intensity (colour code) as a function of time and wave numbers. Representative IR spectra of the two off-gassing components corresponding to the spectrum of MEK at point A, and water at point B.

4.2. Void Formation and Growth

4.2.1. Model input parameters

Figure 4 presents the typical weight gain caused by water molecules diffusion into the uncured polymer network of the adhesive, for various ambient conditions. It is worth noting that, after only 2 hours, water saturation can be reached in the adhesive at relative humidity levels that are not unusually reached if a repair is performed in rainy day. Interestingly, if the ambient air was lower than 30 %RH, the adhesive film could also be dried.

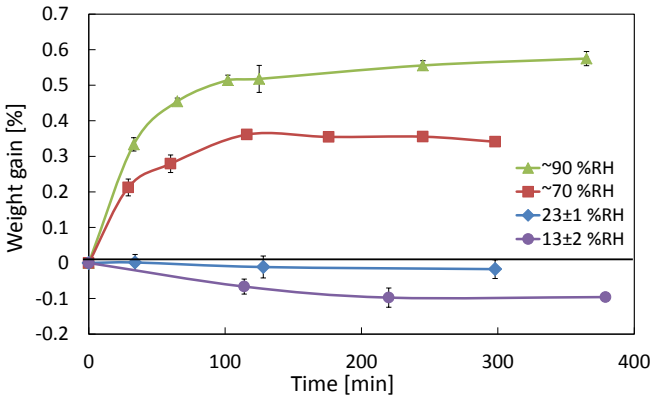

Figure 4: Mass evolution of the uncured adhesive under dry and wet ambient air at 23 °C.

Excerpt from ISBN 978-3-00-053387-7

The calculated diffusion activation energy, 44.5 kJ/mol, is in the order of magnitude of past works on other epoxy systems (between 20 and 60 kJ/mol) [9, 12, 14], and the determined pre-exponential factor 7930 mm^2/min is close to Ledru's measurements [14].

4.2.2. Void Growth Observations and Predictions

In Figure 5, the void growth predictions based on the model of Wood and Bader [11] introduced in section 3.1 are plotted against the measured void content evolving throughout the cure. In this figure, the influence of three levels of pre-cure absorbed moisture is compared to the void formation onset and growth up to gelation. Gel time was determined by the rheological model presented in section 4.1. After gelation, any porosity was trapped within the polymer network, at which point the void growth model and observations were stopped. All of these tests followed the recommended cure cycle (2 °C/min to 121 °C) under full vacuum pressure.

The porosity observations and measurements in Figure 5 showed a strong dependence of the initial water weight content in the adhesive on the final void content. For the baseline (as-received adhesive films), no void nucleation was observed, and void-free adhesive was achieved. For conditioned samples, to up to 0.60 wt. %, the higher the water concentration, the faster voids grew and the larger final voids size and void content were measured. In cases of large areal density of porosity prior to gelation, void coalescence was also observed. The error bars in Figure 5 indicate ± one standard deviation, corresponding to five observations after cure at various locations on the adhesive sample.

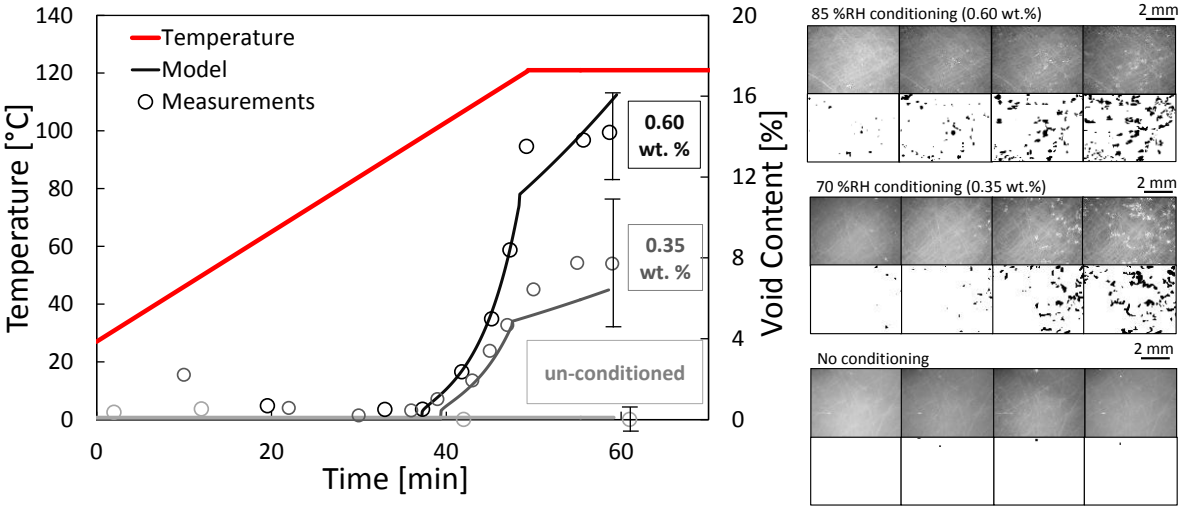

Figure 5: Graph showing the measured and predicted progression of void growth for three different levels of pre-cure absorbed moisture under full vacuum pressure (left). Representative micrographs are displayed along with processed black and white images used to calculate void content (right).

Moreover, the onset of void formation was close to the boiling point of water (96–100 °C) for large amount of absorbed moisture, which was both captured by measurements and the void growth predictions. In light of the unconditioned sample observation, which did not develop any porosity, the presence of MEK did not lead to void nucleation near its boiling point (at 79.6 °C), nor at any other temperature. However, the presence of pre-bond water clearly induced significant void formation and growth.

Another noteworthy observation is related to the change of void growth rate. As soon as the sample reached the hold temperature at 121 °C, void growth rates were found reduced until gelation, at which point the void growth model was stopped. According to this model framework [9, 14], water

Excerpt from ISBN 978-3-00-053387-7

diffusivity, void gas density and water concentration at the void surface are dependent on temperature, and both plateau for a constant temperature. This dependency reduced the rate of void diameter progression, which only slightly increases as a function of time for a constant temperature, similarly to the glass tool-plate observations.

Overall, the analytical model well captured the onset times and temperatures of void formation. Regarding the final void content, a scaling method was used to convert the void diameter predictions into an areal void content, similarly to other researchers [12, 20, 21]. Indeed, since void nucleation, growth and coalescence happen concurrently, a single average void diameter prediction can only scarcely characterize a diverse distribution of porosity, with dozens of voids ranging from a few micros diameters to over 500 µm.

5. Conclusions

The present paper considered the effect of absorbed moisture as the main source of porosity on the void formation and growth under ideal and deficient repair processing conditions. First, TGA-FTIR characterization of the off-gassing species (MEK and water) was carried out. Cytec FM® 300-2M cure kinetic and rheological behaviour and models were also presented. Then, void evolution was monitored under a glass tool-plate throughout the cure of adhesive films with various levels of pre-bond moisture. In parallel, a water diffusion-based void growth model was introduced and used in this study.

In the absence of entrapped air, the results highlighted one critical source of void nucleation: pre-bond moisture. When the repair environment was wet, fast water uptake was measured: up to 0.3 wt. % after only 2 hours under 70 %RH. In such case of absorbed water, it was shown significant void nucleation and growth starting near water boiling point, as well as void coalescence for large void areal content prior to gelation, at which stage any porosity was trapped within the adhesive. Both analytical predictions and experimental measurements were found in close agreement throughout the cure of the adhesive, indicating that the water-diffusion based model is a correct approach to predict moisture-induced void formation in adhesive bonding.

Acknowledgments

The authors are grateful for financial support and materials from the Consortium for Research and Innovation in Aerospace in Quebec (CRIAQ); the Natural Science and Engineering Research Council (NSERC); the Centre de Recherche sur les Systèmes Polymères et Composites à Haute Performance (CREPEC); the National Research Council Canada (NRC/CNRC); Bombardier Aerospace and L-3 MAS. We would like to thank Ms. Marie Romedenne for her support with the adhesive thermo-mechanical analysis, Ms. Marlini Simoes for her help with the glass tool-plate experiments, as well as Dr. Andrea Arias from l'École Polytechnique de Montréal for the guidance with the TGA-FTIR tests.

References

[1] K. B. Katnam, L. F. M. Da Silva, and T. M. Young, "Bonded repair of composite aircraft structures: A review of scientific challenges and opportunities," *Progress in Aerospace Sciences*, vol. 61, pp. 26-42, 2013.

[2] A. MacLean, D. Casari, and P. Hubert, "Wet Layup Composite Bonded Scarf Repairs: Effect of Processing Variables on Porosity," in *SAMPE*, Long Beach, CA, USA, 2016.

[3] L. Salah, "Weak Interfacial Bonds and the Long-Term Durability of Bonded Repairs to Polymer Matrix Composites," PhD, Department of Aerospace Engineering, Wichita State University, Wichita, KS, USA, 2012.

Excerpt from ISBN 978-3-00-053387-7

[4] M. Préau and P. Hubert, "Processing of co-bonded scarf repairs: Void reduction strategies and influence on strength recovery," *Composites Part A: Applied Science and Manufacturing,* vol. 84, pp. 236-245, 2016.
[5] G. N. Sage and W. P. Tiu, "The effect of glue-line voids and inclusions on the fatigue strength of bonded joints in composites," *Composites,* vol. 13, pp. 228-232, 1982.
[6] C. H. Wang and C. N. Duong, "Chapter 10 - Non-destructive evaluation of bond quality," in *Bonded Joints and Repairs to Composite Airframe Structures*, C. H. W. N. Duong, Ed., ed Oxford: Academic Press, 2016, pp. 265-285.
[7] P. J. Pearce, D. R. Arnott, A. Camilleri, M. R. Kindermann, G. I. Mathys, and A. R. Wilson, "Cause and effect of void formation during vacuum bag curing of epoxy film adhesives," *Journal of Adhesion Science and Technology,* vol. 12, pp. 567-584, 1998.
[8] C. Li, R. Ueno, and V. Lefebvre, "Investigation of an accelerated moisture removal approach of a composite aicraft control control surface," N. R. C. Canada, Ed., ed. Ottawa: Society for the Advancement of Material and Process Engineering, 2006.
[9] J. L. Kardos, M. P. Duduković, and R. Dave, "Void growth and resin transport during processing of thermosetting — Matrix composites," in *Epoxy Resins and Composites IV*. vol. 80, K. Dušek, Ed., ed: Springer Berlin Heidelberg, 1986, pp. 101-123.
[10] J. Kratz, "Transport Phenomena in Vacuum Bag Only Prepreg Processing of Honeycomb Sandwich Panels," PhD thesis, Mechanical Engineering, McGill university, 2013.
[11] J. R. Wood and M. G. Bader, "Void control for polymer-matrix composites (1): Theoretical and experimental methods for determining the growth and collapse of gas bubbles," *Composites Manufacturing,* vol. 5, pp. 139-147, 1994.
[12] L. K. Grunenfelder and S. R. Nutt, "Void formation in composite prepregs – Effect of dissolved moisture," *Composites Science and Technology,* vol. 70, pp. 2304-2309, 2010.
[13] P. S. Epstein, "On the Stability of Gas Bubbles in LiquidGas Solutions," *Journal of Chemical Physics,* vol. 18, p. 1505, 1950.
[14] Y. Ledru, G. Bernhart, R. Piquet, F. Schmidt, and L. Michel, "Coupled visco-mechanical and diffusion void growth modelling during composite curing," *Composites Science and Technology,* vol. 70, pp. 2139-2145, 2010.
[15] "BLE Wireless Sensor Tag Demo V1.1," I. Measurement Specialties, Ed., ed: MEAS-SPEC, 2014.
[16] "HTU21D(F) Sensor Datasheet," in *Measurement Specialties, Inc*, ed: MEAS-SPEC, 2014.
[17] C. L. Soles, F. T. Chang, D. W. Gidley, and A. F. Yee, "Contributions of the nanovoid structure to the kinetics of moisture transport in epoxy resins," *Journal of Polymer Science Part B: Polymer Physics,* vol. 38, pp. 776-791, 2000.
[18] K. Cole, J. Hechler, and D. Noel, "A new approach to modeling the cure kinetics of epoxy/amine thermosetting resins. 2. Application to a typical system based on bis [4-(diglycidylamino) phenyl] methane and bis (4-aminophenyl) sulfone," *Macromolecules,* vol. 24, pp. 3098-3110, 1991.
[19] L. Khoun, T. Centea, and P. Hubert, "Characterization Methodology of Thermoset Resins for the Processing of Composite Materials — Case Study: CYCOM 890RTM Epoxy Resin," *Journal of Composite Materials,* vol. 44, pp. 1397-1415, 2010.
[20] F. Y. C. Boey and S. W. Lye, "Void reduction in autoclave processing of thermoset composites: Part 1: High pressure effects on void reduction," *Composites,* vol. 23, pp. 261-265, 1992.
[21] J. P. Anderson and M. C. Altan, "Formation of voids in composite laminates: Coupled effect of moisture content and processing pressure," *Polymer Composites,* vol. 36, pp. 376-384, 2015.

Excerpt from ISBN 978-3-00-053387-7